



INNSPUB

RESEARCH PAPER

Journal of Biodiversity and Environmental Sciences (JBES)

ISSN: 2220-6663 (Print) 2222-3045 (Online)

<http://www.innspub.net>

Vol. 6, No. 2, p. 504-514, 2015

OPEN ACCESS

Characteristics of mineralogy, petrography and textures of rocks in the mata mountain area, South of Jiroft

H. Malek Mohammadi, R. Zarei Sahamiye^{*1}, M. R. Jafari², M. Vossoughi Abedini³

Department of Geology, Science and Research Branch, Islamic Azad University (IAU), Teheran, Iran

¹*Department of Geology, Lorestan University, Lorestan, Iran*

²*Department of Geology, Tehran branch, Islamic Azad University (IAU), Tehran, Iran*

³*Department of Geology, Science and Research Branch, Islamic Azad University (IAU), Tehran, Iran*

Article published on February 09, 2015

Key words: Jiroft, Diabase, Ophitic, Porphyric texture, Intersertal.

Abstract

South Jiroft rocks in the Mata mountain area of mineralogy and chemical composition divided to three groups: basalt, gabbro and diabase. The age of these rocks is attributed to the lower Jurassic. The study area is located in 75 km from SW of Jiroft in Kerman province and the Mata village is the closest village to it. The basalts contain pyroxene and plagioclase. These basaltic rocks have a porphyric texture with microlitic to glass matrix. The second type of rock in the study area is diabas and its mineralogy including pyroxene and plagioclase. These rocks have intergranular and intersertal texture. The third type of rocks in this area, in terms of petrography is ophitic gabbro with mineralogy including pyroxene, plagioclase and minor minerals. The texture of this gabbro is porphyric texture with medium-grained matrix.

***Corresponding Author:** R. Zarei Sahamiye ✉ Zareisah@yahoo.com

Introduction

The study area is a part of sedimentary - igneous basin and Sanandaj - Sirjan that belongs to the Jurassic - Cretaceous. In the extreme of Sanandaj - Sirjan zone (Sargaz – Mata area), the volcanoclastic, mafic and felsic igneous rocks are exposed. Given the stratigraphic relationships, the age of these rocks has been attributed to the lower Jurassic (1:250 000 Sabzevaran Map and 1:100000 Esfandaghe, Mohamadabad and Sabzevaran Map).

This tectonic zone is a failed crevasse and is considered as a part of the Zagros in previous studies. Sanandaj-Sirjan is a narrow zone with about 1500 km length and 250-150 km width and is located between Sirjan-Esfandaghe cities in the SE and Sirjan-Oromiye cities in the NW. The study area is a part of sedimentary - igneous basin and Sanandaj - Sirjan that belongs to the Jurassic - Cretaceous. Mesozoic sediments in this basin can be divided into two main sections.

This area has the NW- SE trend and continues from the West of Lake Oromiye to SE of fault prison. In the

Sanandaj-Sirjan Zone, Magmatism and tectonic phases have occurred in the highest value. So this zone is considered the most troubled and most tectonic zones of Iran.

The study area is classified semi-arid regions. This region has a temperate spring and autumn, heat summer and cold and dry winter. The rainfall is less than 200 mm in this region. The average annual temperature is 28 centigrade degrees that temperatures in summer reach over 40 degrees. Sanandaj-Sirjan zone are located in S and SW of central Iran and NE of the Zagros zone and is limited to the north by Oromiye - Doughter and to the SW by the Zagros folded thrust belt.

The study area is located in 75 kilometers South-West of Jiroft in Kerman province and the Mata village (20 km SW of Karim Abad) is the closest village to it. It geographic location is between 57°27 - 57°28 and 28°22 - 28°23 (Fig. 1). This region has a relatively gentle topography.

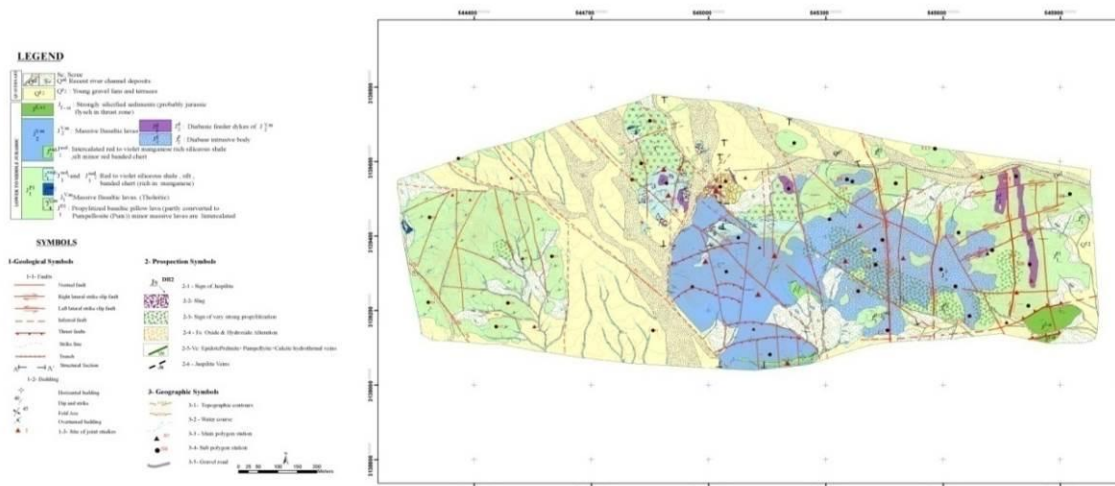


Fig. 1. Geographic location and access to the Siah Mine Mountain (Atlas of Iran Road).

Its prominent ridge mainly formed from basalt igneous rocks and the low-lying areas have formed from the fililshs complex of lower- middle Jurassic. fililshs complex are erodible and generally make up the sinking area. A network of waterways is with the

general NW - SE trend in this region. N-S dyke (with a basaltic composition) are interesting morphological features in this region that as prominent walls are exposed within the fililshs complex and pillow lavas. Rocks of mineralogy and chemical composition divide

in three groups of basalt, ophitic gabbro and diabase in the study area.

preparation and was studied with polarizing microscope.

The aim of this paper is characteristics of mineralogy, petrography and textures of rocks in the mata mountain area in south of Jiroft, Kerman province.

15 samples was the chemical analysis by the XRF, XRD method in central lab Tehran University (in Iran) and 15 samples with ICP-MS method in ACME Labs (in Canada) (Table 1 and 2).

Materials and methods

Sampling and analysis method

During the field observations was collected of 150 rock samples from two parts of the study area. After studying the manual sample, 125 thin section

Also the results abating from these analysis were used for drawing charts by different soft wares especially Excel, Minpet, Igpert and Photoshop and Corel Drow were used for analysis and drawing charts.

Table 1. Chemical analysis data of the main oxides with ICP-MS method.

	SiO ₂	TiO ₂	Al ₂ O ₃	Fe ₂ O ₃	MnO	MgO	CaO	Na ₂ O	K ₂ O	P ₂ O ₅	LOI	Sum
9821	48.44	1.06	13.58	11.45	0.15	8.34	9.39	3.66	0.43	0.10	3.61	100.21
9824	48.16	1.05	15.17	11.70	0.18	7.22	10.43	2.55	0.17	0.09	4.22	100.94
9829	42.66	0.25	5.20	6.55	0.13	3.04	35.22	0.24	0.06	0.27	6.84	100.46
9837	49.28	0.92	15.46	10.89	0.20	7.02	10.40	2.78	0.57	0.08	4.40	102.01
9839	49.55	0.89	16.13	10.38	0.19	6.88	10.21	2.83	0.48	0.08	4.83	102.46
9842	50.26	1.28	14.53	13.41	0.22	6.36	8.94	3.94	0.23	0.11	3.26	102.54
9845	48.80	1.23	14.24	13.23	0.21	6.07	9.63	3.16	0.14	0.12	4.71	101.54
9848	49.39	1.45	14.51	14.78	0.23	5.54	7.85	4.00	0.25	0.13	3.13	101.26
10107	45.78	0.44	8.84	8.31	0.25	3.21	23.70	1.89	0.43	0.33	6.03	99.20
10109	45.86	0.25	5.21	6.53	0.13	1.96	31.41	0.22	0.05	0.26	6.81	98.68
10102	45.80	0.43	8.74	8.23	0.23	3.20	23.50	1.88	0.33	0.23	6.02	98.59
10206	47.61	1.02	15.09	11.26	0.20	6.66	10.13	2.91	0.42	0.10	4.85	100.25
10209	47.94	0.99	15.13	10.80	0.21	6.40	9.92	3.28	0.39	0.10	4.71	99.86
10213	48.07	0.99	14.94	10.79	0.22	6.07	10.14	2.49	0.35	0.10	5.87	100.03
10104	44.80	0.33	8.54	8.13	0.22	3.40	22.50	1.87	0.24	0.13	6.12	96.28

Table 2. Chemical analysis data of the trace element with ICP-MS method.

	V	Cr	Co	Ni	Cu	Zn	Rb	Sr	Y	Zr	Nb	Ba	Pb	Th
9821	334	111	4739	76	154	84	38	139	35	149	31	65	8	3.3
9824	326	89	48.2	73	144	84	42	127	35	151	30	85	9	3.4
9829	327	48	52.0	74	804	103	40	10	37	153	32	38	34	7.2
9837	313	74	45.1	65	198	78	33	200	28	123	29	188	8	4.2
9839	301	61	43.4	59	193	75	35	194	28	124	28	144	8	3.7
9842	408	17	51.4	34	204	85	35	147	36	106	29	56	9	3.5
9845	394	16	50.0	31	120	94	32	83	39	154	29	24	9	3.3
9848	465	12	53.8	26	133	115	37	143	40	165	31	46	19	3.3
10107	195	33	28.8	51	72	50	28	34	28	133	20	65	32	5.6
10109	144	19	23.5	30	241	55	25	18	17	90	11	4	40	3.4
10102	194	32	28.7	50	62	40	29	35	27	129	18	62	30	5.3
10206	321	75	45.5	57	103	85	35	172	31	109	28	89	9	3.3
10209	303	83	43.4	56	128	74	31	162	29	98	26	83	8	3.4
10213	308	80	43.9	59	127	86	39	141	31	99	28	96	8	3.7
10104	184	29	27.7	49	59	48	28	29	26	121	20	59	29	5.2

Table 2. Chemical analysis data of the trace element with ICP-MS method.

	La	Ce	Nd	Sm	Eu	Tb	Yb	Lu	Cs	Hf	Ta	Dy	Er	U	W
9821	5	10	31.4	5.67	1.63	0.66	4.4	0.32	3.2	6.0	0.80	3.39	2.00	5.0	1.03
9824	4	9	30.5	5.21	1.70	0.62	4.4	0.27	2.7	5.7	0.59	3.14	1.85	5.0	0.98
9829	32	43	35.1	6.53	1.65	0.77	4.1	0.29	3.1	5.2	0.70	3.67	2.06	3.9	3.78
9837	4	8	29.1	5.49	1.56	0.66	3.8	0.25	3.2	4.9	0.80	3.36	1.92	4.8	0.99
9839	4	8	29.6	5.62	1.54	0.65	3.7	0.25	2.5	4.7	0.70	3.20	1.84	4.8	0.98
9842	4	10	30.5	5.44	1.66	0.65	4.7	0.30	2.7	5.6	0.85	3.27	1.93	5.5	0.97
9845	4	10	31.7	5.88	1.62	0.72	4.9	0.27	3.0	5.2	0.75	3.58	2.08	5.1	1.05
9848	5	11	32.2	5.87	1.63	0.70	5.1	0.27	3.2	5.2	0.80	3.56	2.08	5.2	0.99
10107	22	28	33.4	6.16	1.78	0.77	3.4	0.40	2.7	5.3	0.70	3.90	2.16	4.5	1.09
10109	14	14	33.4	6.19	1.80	0.75	2.5	0.28	2.6	5.3	0.80	3.66	2.09	3.9	1.02
10102	19	27	33.3	6.15	1.68	0.78	3.3	0.50	2.6	5.2	0.60	3.80	2.15	4.6	1.06
10206	4	9	29.9	5.65	1.40	0.66	3.9	0.27	2.6	4.7	0.80	3.32	1.88	5.0	1.11
10209	4	9	29.4	5.10	1.63	0.59	3.7	0.24	2.2	5.4	0.90	2.99	1.82	4.9	0.97
10213	4	9	36.9	6.75	1.81	0.78	3.9	0.23	2.7	5.3	0.80	3.87	2.18	5.0	1.00
10104	18	26	32.4	6.26	1.76	0.68	3.2	0.40	2.4	4.3	0.70	3.70	2.12	4.4	1.05

Results and discussions

Geology of atudy area

Sanandaj-Sirjan zone is limited to the north by Oromiye - Doughter and to the SW by the Zagros folded thrust belt and are located in S and SW of central Iran and NE of the Zagros zone and. This tectonic zone is a failed crevasse and is considered as a part of the Zagros in previous studies. Sanandaj-Sirjan is a narrow zone with about 1500 km length and 250-150 km width and is located between Sirjan-Esfandaghe cities in the SE and Sirjan-Oromiye cities in the NW. This area has the NW- SE trend and continues from the West of Lake Oromiye to SE of fault prison. In the Sanandaj-Sirjan Zone, Magmatism and tectonic phases have occurred in the highest value. So this zone is considered the most troubled and most tectonic zones of Iran.

In the extreme of Sanandaj - Sirjan zone (Sargaz – Mata area), the volcanoclastic, mafic and felsic igneous rocks are exposed. Given the stratigraphic relationships, the age of these rocks has been attributed to the lower Jurassic (1:250 000 Sabzevaran Map and 1:100000 Esfandaghe, Mohamadabad and Sabzevaran Map).

The study area is a part of sedimentary - igneous basin and Sanandaj - Sirjan that belongs to the

Jurassic - Cretaceous. Mesozoic sediments in this basin can be divided into two main sections:

1- Turbidite – filishs deposits in the lower - middle Jurassic and volcanic rocks associated with it. These sets have been deposited on the Paleozoic metamorphic in Sanandaj – Sirjan zone. Magmatic activities of this part are as pillow lavas and basaltic dense lava that very few felsic rocks are accompanied in the northern part of the basalts. Basic dykes (diabasic) as Swarm Dyke cooperation this part with along the North – South.

2- Calpionella limestone has been deposited with specified angle on the igneous - sedimentary complex of part 1. The age of these limestones was Upper Jurassic to Lower Cretaceous and in some parts around of this complex, gradually changes to Lower Cretaceous limestone. Volcanic activity is not seen in any way in this limestone and can be firmly said that volcanic activity occurred in the period between the Lower to middle Jurassic. The study area is located in the Zagros - Makran transfer zone and important part of the Oman line. This area is active zone. This activity works follow up with the morphological evidence and the earthquakes that occurred in the region.

Tectonic Setting

This region is located at the crossroad of strike slip fault system. One of the fault systems is with the North- South line and mechanisms are related to the performance of Zagros - Makran zone and other fault system is along the N060 and mechanisms are left. Also, there has been a West - East pressure system in different parts of the region. Faults are developed in three major fault systems (Fig. 2);

- 1 - Left strike-slip faults along the NE -SW (about N060).
- 2 - Right strike-slip faults along the N-S to NW-SE (Fig. 3).
- 3 - Drift fault with the E-W trend.

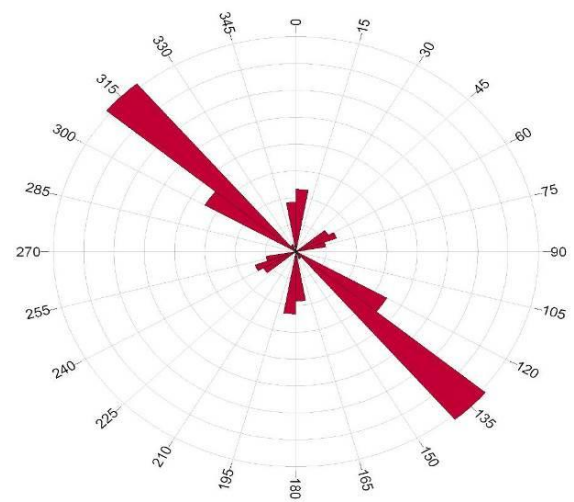


Fig. 2. Faults in the map diagram.



Fig. 3. A) Right strike-slip faults along the N-S, images from the East. B) Right strike-slip faults in the eastern part of the study area, images from the SE.

The joints have been looked in the range of about 14 stations. Based on the adaptive between joints navigation with faults systems, can be said that the more joint development in the region are associated with the fault zone. The main joints are almost parallel along the main fault zone and some of them are associated with P, R, R / fractures in the fault zone and have been created with certain angles to the main line. The joints with N060 direction are abundant joints developed in most stations that associated with strike-slip fault zone. Determine the relative age of the joints in the station number 9, shows this system is the youngest fracture system in the study area (Fig. 4).



Fig. 4. Image of the joint station number 9, Note to the three perpendicular joints systems and a delay system with the N-W direction (N060).

Petrography

Petrographically, one group of rocks in the study area is basalts and its combination has pyroxene phenocrysts, plagioclase and matrix.

- Pyroxene

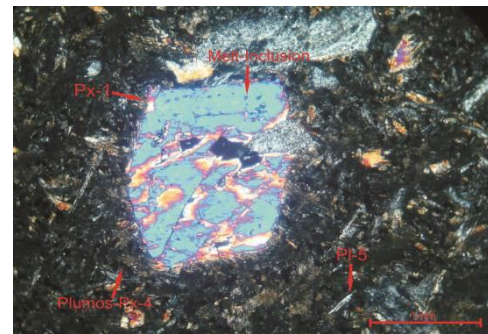
The pyroxene can be seen in the field as subhedral to euhedral. Based on the optical properties, these pyroxenes are augite and diopside type (Shelly 1993). In some cases, these minerals have been replaced by prehnite and calcite. Pyroxene micro phenocrysts minerals are viewed with radial morphology and in a different direction. Pyroxenes are observed to four different species (Fig. 5):

1- Single crystal pyroxene, which can be seen as subhedral to euhedral with an average size 500µm that scattered in the field (Px-1). From features can be mentioned to the incorporation of melted in the near edge of the minerals. The fiber pyroxene with fine plagioclase can be seen on these pyroxenes.

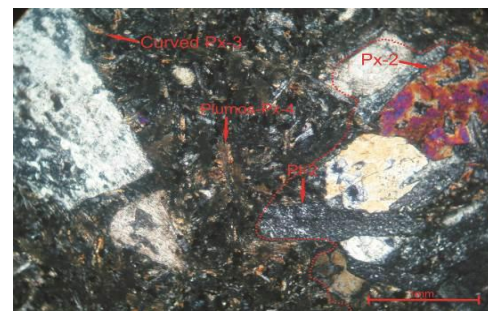
2- The cluster pyroxenes can be seen along with plagioclase (Px-2). These pyroxenes are seen euhedral to subhedral and and can be seen with average size 150 µm. These pyroxenes created by subtracting in the lower part of magma reservoir that is reached to the top by changes in the reservoir (Shelley 1993).

3 – Pyroxenes with curved and flat micromorphology (Px-3). These pyroxenes based on the optical properties are augite. They can be observed in the nature.

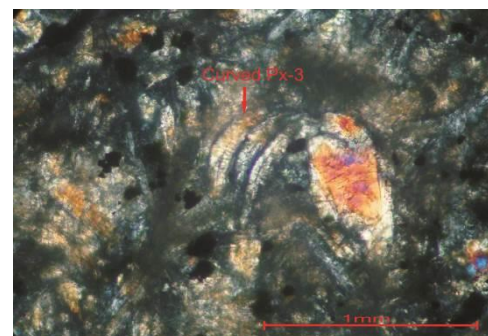
4 - Pyroxenes growth with microlite of plagioclase or independently of the skeletal micromorphology and are observed of microphenocryst with spherulitic micromorphology (dendritic, fan and bow) (Px-4). The core of these pyroxenes has been made on the plagioclase and pre-formed pyroxene. These infrastructures are rapidly cooled margins (Bouquain *et al*, 2009; Christopher *et al*, 2005; Fowler *et al*, 2002; Jafri *et al*, 1992).



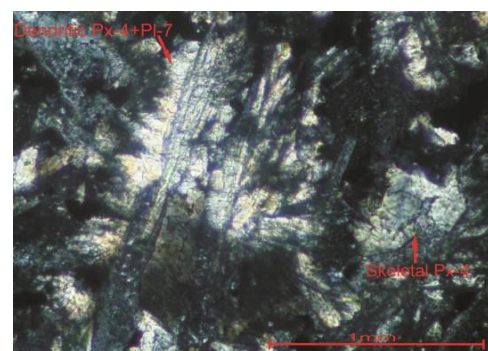
(A)



(B)



(C)



(D)

Fig. 5. A) phenocrysts of the first type of pyroxene (diopside) with the melt incorporation in the margins and fourth type of pyroxene in XPL. B) Second type of pyroxene with plagioclase that is created cluster infrastructure in XPL. C) The third type of pyroxene in XPL. D) The fourth type of pyroxene that is skeletal and dendritic in XPL.

- Plagioclase

Plagioclase crystals are often euhedral to subhedral and can be seen with size 50 μm to 1.2 mm in the rock. Some of these plagioclases have albite – Karlsbad, albite - Pryklin twins and zoning. Based on optical properties, the maximum angle of extinction and refraction, these plagioclases are andazine to labradorite. Most plagioclases have been altered to secondary minerals. Most of them are sericity and clay minerals. Seven different types of plagioclase can be seen in these basalts (Fig. 6) (Seaman, 2000):

1 - Plagioclase in the form of mass crystals and are composed of more than two plagioclase minerals (Pl-1). From its features can be mentioned to congresses crystalline between boundaries. In the surrounding of them can be seen dissolution zone of imbalance.

2 - The cluster plagioclase made up the community of plagioclase and pyroxene. The alteration of them is more than mass plagioclase (Pl-2).

3 - The single crystals of mass plagioclase have the melt incorporation with the simple honeycomb in the core and margins. From the imbalance infrastructure can be related to the gulf infrastructure and the dissolution zone. This melt incorporation has been altered to the clay minerals (Pl-3).

4 - Plagioclases without incorporation are in the field of rock (Pl-4).

5 - Plagioclases in the form of microlite are observed with different sizes in the field (Pl-5).

6 - Plagioclases with zoning region which has drastically altered. Such plagioclase has a low abundance of other species of them. From its features can be noted to dissolution margin (Pl-6) (Rigopoulos *et al*, 2010).

7 - Plagioclases and pyroxene and can be observed in the radius and the root form (Pl-7). The infrastructure is changed between 50 - 200 μm .

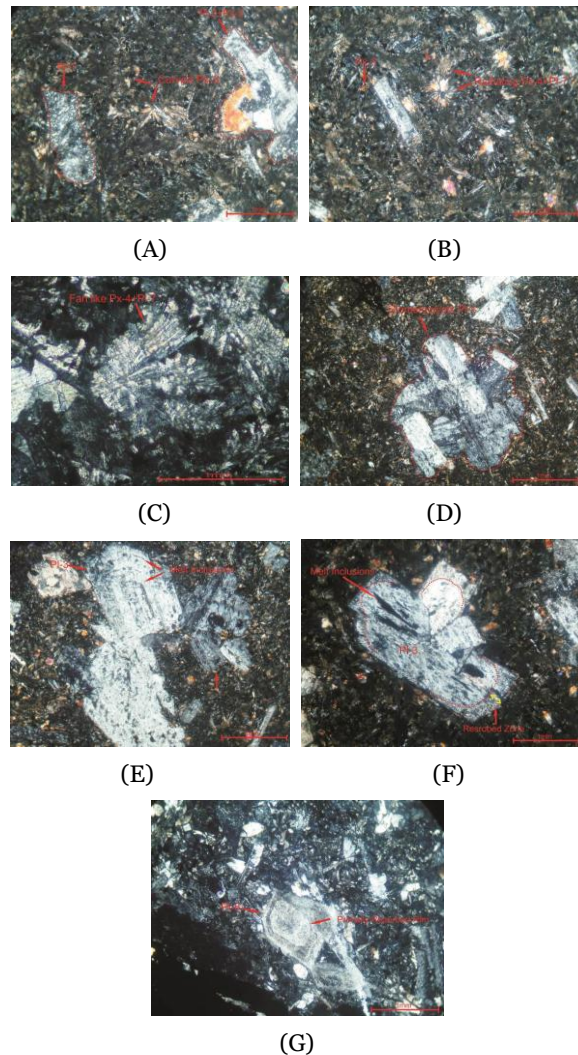


Fig. 6. A) The first type of plagioclase, bend pyroxene and the cluster infrastructure (the red china) in XPL. B) The fourth species of pyroxene and seventh type of plagioclase that are seen with radial micromorphology in XPL. C) The fourth species of pyroxene and seventh type of plagioclase with fan micromorphology in XPL. D) The mass plagioclase in XPL. E) The third type of plagioclase with melt incorporation and gulf infrastructure (red arrow) in XPL. F) The third type of plagioclase with infrastructure and the dissolution zone in XPL. H) The sixth type of plagioclase with oscillatory zoning and dissolution border in XPL.

- Nature

Nature of the glass (which has been completely replaced by clay minerals) is composed of plagioclase microlites, clinopyroxene with radial morphology and

opaque minerals. Plagioclase microlites are often altered to calcite and serisit.

In basalt of this region are observed the mixing components of volcanoclasts. Given the evidence such as enter the plagioclase microlites and pyroxene crystals from the host rock into the clot, also margins are rapidly cooled around the clot, it can be concluded that pyroclastic clots is inserted to basalt before the final cooling.

- Second group of Mata rocks, of petrography is diabase and its combination has pyroxene and plagioclase phenocrystals. This diabase texture is intergranular and intersertal.

- *Pyroxene*

The pyroxene can be seen in the field as subhedral to euhedral with size between 20µm – 1.3 mm. Based on the optical properties, these pyroxenes are augite to diopside type. The infrastructure created by these minerals, can be related to ophitic, subophitic, inter granular (Rigopoulos *et al*, 2010). These minerals in some cases have been replaced by prehnite, chlorite, actinolite and calcite. In this diabase can see three different species of pyroxene (Fig. 7).

1- Single crystal pyroxene can be seen as subhedral to euhedral with an average size 100 µm in plagioclase (Px-1). This pyroxene have created intergranular infrastructure.

2 - Pyroxene with incorporation of plagioclase is observed in the rock with size between 200µm – 1.3 mm (Px-2). These pyroxenes often have a diopside combination that after subtraction of the magma reservoir in the lower part, has reached to the top by changes within the reservoir (Rigopoulos *et al*, 2010).

3 - Pyroxene that have branching micromorphology and is observed with low dispersion by size between 100µm - 400µm (Px-3). Based on the optical properties, these are diopside type. These species of pyroxene are observed in the nature.

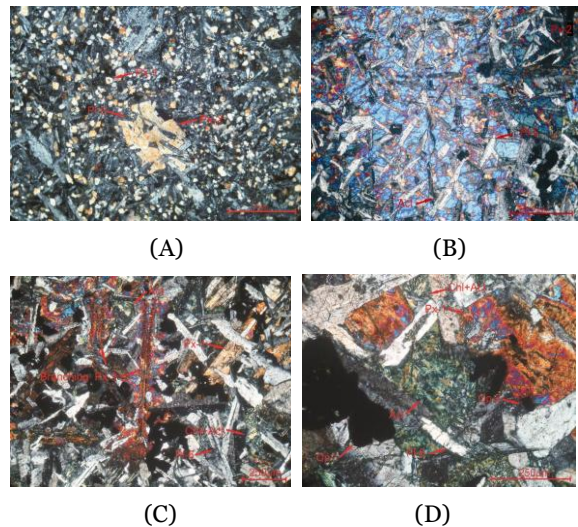


Fig. 7. A) The first and second species of pyroxene with ophitic and subophitic infrastructure in XPL. B) View of ophitic infrastructure (second species of pyroxene) in XPL. C) The first species and the third branching types of pyroxene in XPL. D) Another view of the first species of pyroxene, chlorite and actinolite is in the spaces between the sixth plagioclases in XPL.

- *Plagioclase*

Plagioclases can be seen as euhedral to unhedral with an average size 170 µm – 1.5 mm. From features of them can be noted to albite - karlsbad and albite – peryklin twin. Based on optical properties such as the maximum angle of extinction and refraction factor, these plagioclases are andazine to labradorit. serisytt and clay minerals are the alteration products of these minerals. Six species of plagioclase can be observed in this diabase (Seaman, 2000) (Fig 8).

1- The mass crystals of plagioclases are composed from a community of over two minerals (Pl-1). From its features can be mentioned to congress crystalline bonder. More calcic plagioclase can be seen around the plagioclase. Of created infrastructure can be mentioned to the dissolution infrastructure (Arndt *et al*, 2008).

2 – The cluster plagioclase that is composed from the community of plagioclase and pyroxene (Pl-2).

3 - A honeycomb form plagioclase that has melt incorporation. These melt incorporation have been altered to clay minerals (Pl-3).

4 - Plagioclase without incorporation is observed in the rock (Pl-4).

5 - Microlite of plagioclase within the pyroxene is seen with ophitic and subophitic tissue (Nomade *et al.*, 2002)(Pl-5).

6 - Microlite of plagioclase is observed within the field (Pl-6).

Accordingly, the mass or cluster plagioclase is the remaining remnants from komolite layers (Seaman, 2000).

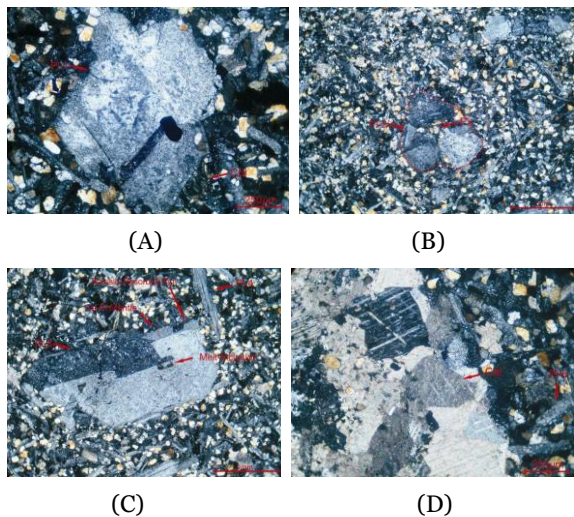


Fig. 8. A) View of the mass plagioclase in XPL. B) View of the cluster plagioclase with pyroxene in XPL. C) The third type of plagioclase with melt incorporation and dissolve infrastructure and fourth specie of plagioclase in XPL. D) Microlite of plagioclase and calcite with second and third twin in XPL.

- Nature

The nature is composed of the recrystalline glass (string chlorite from penin type, fiber amphibole from actinolite and plagonit type), microlite of plagioclase, clinopyroxene and opaque minerals. Microlite of plagioclase often have altered to serisyt. The

intergranular and intersertal tissue created by this microlites (Vernon *et al.*, 2004). Minor minerals include opaque (Op-1) which is subhedral to unihedral and in some cases are scattered as skeletal and fine grained in the rock. Of the other minerals can be noted to calcite with the average size 100µm. The calcite is in the unihedral shape and in some cases can be observed with the second and third type twin. The secondary alteration minerals are chlorite, serisyt, calcite, biotite and opaque minerals (Op-2) (Bear *et al.*, 2007).

- Third group of Mata rocks, of petrography is ophitic gabbro and its combination has pyroxene and plagioclase phenocrystals and Minor minerals. This ophitic gabbro has porphyric texture (Fig 9).

- Pyroxene

Pyroxene is observed as euhedral to unihedral with an average size 500 µm – 1.2 mm in the rock. Based on the optical properties, these pyroxenes are augite and diopside type.

The infrastructures that can be caused by these minerals are ophitic and subophitic infrastructure. The products of this pyroxene are actinolite, chlorite and opaque minerals.

- Plagioclase

Plagioclase is observed as euhedral to unihedral with albite and albite – karlsbad twin. Based on optical properties such as the maximum angle of extinction and refraction factor, these plagioclases are andazine to labradorit. The alteration products of these minerals are serisyt and clay minerals.

- Minor Minerals

Minor minerals include opaque minerals (Op-1) (these are scattered as subhedral to unihedral with an average size 50 µm – 250 mm in the rock), primary amphibole (based on the optical properties is hornblende and in some cases have become biotite), alkali feldspar (they can be seen with karlsbad twin and low dispersion as incorporation in the pyroxene

and in the rock), Chlorite and actinolite (have been formed in the space between the other minerals).

- The secondary minerals

The secondary minerals that result from the alteration include chlorite, actinolite, sersysyt, biotite, clay minerals and opaque minerals (Op-2).

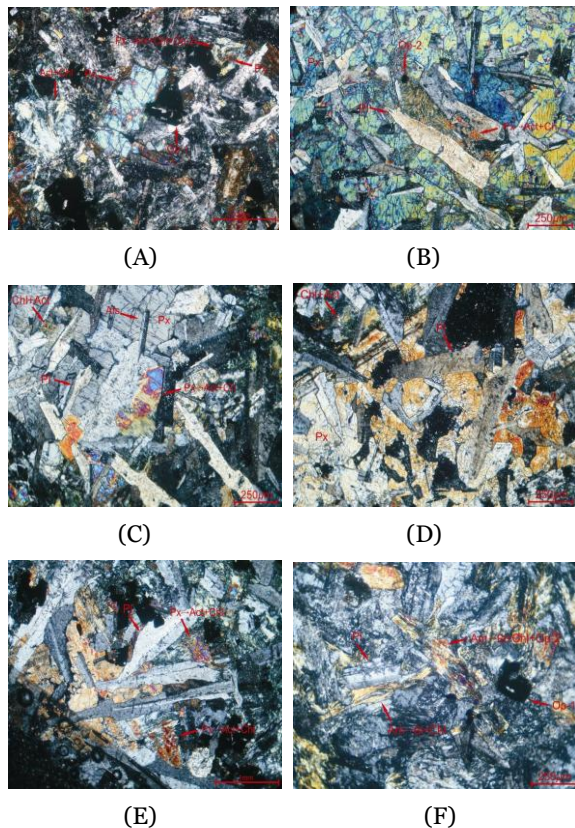


Fig. 9. A) Diopside, altered pyroxene, chlorite and actinolite form in the free space in XPL. B) A view of an ophitic infrastructure that is altered to chlorite, opaque minerals (Op-2) and actinolite in XPL. Due to the alteration of pyroxene. C) Another view of the ophitic incorporation with alkali feldspar and plagioclase incorporation in XPL. D) A view of augite and plagioclase in XPL. E) A view of the elongated crystals of plagioclase in pyroxene (ophitic and subophitic infrastructure) in XPL. F) A view of the amphibole altered to biotite, chlorite and opaque minerals (Op-2) in XPL.

Conclusion

Rocks of mineralogy and chemical composition divide in three groups of basalt, ophitic gabbro and diabase

in the study area. The basalts contain pyroxene and plagioclase. These basaltic rocks have a porphyric texture with microlitic to glass matrix. The pyroxene can be seen as subhedral to euhedral in the field. Based on the optical properties, these pyroxenes are augite and diopside type. Pyroxenes are observed to four different species. The plagioclase can be seen as euhedral to unhedral with an average size 50 μm – 1.2 mm in the field. These plagioclases are andazine to labradorit type (Shelley 1993). Plagioclases are observed to seven different species. Nature is composed of the glass, plagioclase microlites, clinopyroxene with special morphology and opaque minerals. The second type of rock in the study area is diabases and its mineralogy including pyroxene and plagioclase. These rocks have intergranular and intersertal texture. The pyroxene can be seen in the field as subhedral to euhedral with size between 20 μm – 1.3 mm. Based on the optical properties, these pyroxenes are augite to diopside type. Pyroxenes are observed to third different species. Plagioclase crystals are often euhedral to unhedral and can be seen with size 170 μm to 1.5 mm in the rock. These plagioclases are andazine to labradorite. Six different types of plagioclase can be seen in these rocks. The nature is composed of the recrystalline glass, microlite of plagioclase, clinopyroxene and opaque minerals. The third type of rocks in this area, in terms of petrography is ophitic gabbro with mineralogy including pyroxene, plagioclase and minor minerals. The texture of this gabbro is porphyric texture with medium-grained matrix. The pyroxene can be seen in the field as subhedral to unhedral with size between 500 μm – 1.2 mm. Based on the optical properties, these pyroxenes are augite to diopside type. Plagioclase crystals are often euhedral to unhedral with albite and albite – karlsbad twin. They are andazine to labradorit type.

References

Arndt N, Leshner CM, Barnes SJ. 2008. Komatiite Cambridge.

Bear AN, Cas RAF. 2007. The complex facies architecture and emplacement sequence of a Miocene submarine mega-pillow lava flow system. Muriwai. North Island. New Zealand. Journal of Volcanology and geothermal research **160(2)**, 1-22.

Bouquain S, Arndt NT, Hellebrand E. 2009. Crystallochemistry and origin of pyroxenes in komatiites. Contrib mineral petrol **158(1)**, 599-617.

Christopher O, Winter JD. 2005. The occurrence, vesiculation, and solidification of dense blue glassy pahoehoe. Journal of Volcanology and Geothermal Research **142(3)**, 285-301.

Fowler AD, Beger B, Shore M, Jones MI, Ropchan J. 2002. Supercooled rocks: development and significance of varioles spherulites.

Jafri SH, Charan SN. 1992. Quench textures in pillow basalt from the Andamn-Nicobar Islands, Bay of Bengal, India. earth planet Sci **101(1)**, 99-107.

Nomande S, Pouclet A, Chen Y. 2002. The French Guyana doleritic dykes; geochemical evidence

of three populations and new data for the Jurassic central Atlantic magmatic province. Journal of geodynamics **34(2)**, 595-614.

Rigopoulos I, Tsikouras B, Pomonis P, Hatzipanagiotou K. 2010. The influence of alteration on the engineering properties of dolerites: the examples from the Pindos and Vourinos ophiolites (northern Greece). international journal of rock mechanics & mining sciences **47(3)**, 69-80.

Seaman SJ. 2000. Crystal clusters, Feldspar glomerocrysts and magma envelopes in the Atascoa Lookout lava flow. Sothern Arizona. USA: Records of magmatic events. Journal of Petrology **5(2)**, 693-716.

Shelly D. 1993. Igneous and metamorphic rocks under the microscope. Chapman and Hall. London 630p.

Shelly D. 1993. Microscopic study of Igneous and Metamorphic rock. Champan and Hall. London 184p.

Vernon RH. 2004. A practical guide to rock microstructures. Cambridge. England.